nature

https://doi.org/10.1038/d41586-021-03824-5

Accelerated Article Preview

Omicron extensively but incompletely escapes Pfizer BNT162b2 neutralization

Received: 14 December 2021

Accepted: 23 December 2021

Accelerated Article Preview Published online: 23 December 2021

Cite this article as: Cele, S. et al. Omicron extensively but incompletely escapes Pfizer BNT162b2 neutralization. *Nature* https://doi.org/10.1038/d41586-021-03824-5 (2021).

Sandile Cele, Laurelle Jackson, David S. Khoury, Khadija Khan, Thandeka Moyo-Gwete, Houriiyah Tegally, James Emmanuel San, Deborah Cromer , Cathrine Scheepers, Daniel Amoako , Farina Karim, Mallory Bernstein , Gila Lustig, Derseree Archary, Muneerah Smith, Yashica Ganga, Zesuliwe Jule, Kajal Reedoy, Shi-Hsia Hwa, Jennifer Giandhari, Jonathan M. Blackburn, Bernadett I. Gosnell, Salim S. Abdool Karim, Willem Hanekom, NGS-S, COMMIT-KZN Team, Anne von Gottberg, Jinal Bhiman, Richard J. Lessells, Mahomed-Yunus S. Moosa, Miles P. Davenport , Tulio de Oliveira, Penny L. Moore & Alex Sigal

Omicron extensively but incompletely escapes Pfizer BNT162b2 neutralization

Sandile Cele[1,2], Laurelle Jackson[1], David S. Khoury[3], Khadija Khan[1,2], Thandeka Moyo-Gwete[4,5], Houriiyah Tegally[6,7], James Emmanuel San[6], Deborah Cromer[3], Cathrine Scheepers[4,5], Daniel G. Amoako[2,4], Farina Karim[1,2], Mallory Bernstein[1], Gila Lustig[8], Derseree Archary[8,9], Muneerah Smith[10], Yashica Ganga[1], Zesuliwe Jule[1], Kajal Reedoy[1], Shi-Hsia Hwa[1,11], Jennifer Giandhari[6], Jonathan M. Blackburn[10,12], Bernadett I. Gosnell[13], Salim S. Abdool Karim[8,14], Willem Hanekom[1,11], NGS-SA[§], COMMIT-KZN Team[§§], Anne von Gottberg[4,5], Jinal N. Bhiman[4,5], Richard J. Lessells[6,8], Mahomed-Yunus S. Moosa[13], Miles P. Davenport[3], Tulio de Oliveira[6,7,8,15], Penny L. Moore[4,5,8,12], Alex Sigal[1,2,16*]

[1]Africa Health Research Institute, Durban, South Africa. [2]School of Laboratory Medicine and Medical Sciences, University of KwaZulu-Natal, Durban, South Africa. [3]Kirby Institute, University of New South Wales, Sydney, Australia. [4]National Institute for Communicable Diseases of the National Health Laboratory Service, Johannesburg, South Africa. [5]SA MRC Antibody Immunity Research Unit, School of Pathology, Faculty of Health Sciences, University of the Witwatersrand, Johannesburg, South Africa. [6]KwaZulu-Natal Research Innovation and Sequencing Platform, Durban, South Africa. [7]Centre for Epidemic Response and Innovation, School of Data Science and Computational Thinking, Stellenbosch University, Stellenbosch, South Africa. [8]Centre for the AIDS Programme of Research in South Africa, Durban, South Africa. [9]Department of Medical Microbiology, University of KwaZulu-Natal, Durban, South Africa [10]Department of Integrative Biomedical Sciences, Faculty of Health Sciences, University of Cape Town, Cape Town, South Africa. [11]Division of Infection and Immunity, University College London, London, UK. [12]Institute of Infectious Disease and Molecular Medicine, University of Cape Town, Cape Town, South Africa.[13]Department of Infectious Diseases, Nelson R. Mandela School of Clinical Medicine, University of KwaZulu-Natal, Durban, South Africa. [14]Department of Epidemiology, Mailman School of Public Health, Columbia University, New York, NY, United States [15]Department of Global Health, University of Washington, Seattle, USA. [16]Max Planck Institute for Infection Biology, Berlin, Germany.

* Corresponding author. Email: alex.sigal@ahri.org

The emergence of Omicron (Pango lineage B.1.1.529), first identified in Botswana and South Africa, may compromise vaccine effectiveness and lead to re-infections[1]. We investigated whether Omicron escapes antibody neutralization in South Africans vaccinated with Pfizer BNT162b2. We also investigated if Omicron requires the ACE2 receptor to infect cells. We isolated and sequence confirmed live Omicron virus from an infected person in South Africa and compared plasma neutralization of Omicron relative to an ancestral SARS-CoV-2 strain, observing that Omicron still required ACE2 to infect. For neutralization, blood samples were taken soon after vaccination from participants who were vaccinated and previously infected or vaccinated with no evidence of previous infection. Neutralization of ancestral virus was much higher in infected and vaccinated versus vaccinated only participants but both groups showed a 22-fold escape from vaccine elicited neutralization by the Omicron variant. However, in the previously infected and vaccinated group, the level of residual neutralization of Omicron was similar to the level of neutralization of ancestral virus observed in the vaccination only group. These data support the notion that, provided high neutralization capacity is elicited by vaccination/boosting approaches, reasonable effectiveness against Omicron may be maintained.

The emergence of the Omicron variant of SARS-CoV-2 in November 2021 in South Africa and Botswana was first described in South Africa (https://www.nicd.ac.za/wp-content/uploads/2021/11/Update-of-SA-sequencing-data-from-GISAID-26-Nov_Final.pdf) and transmission was rapidly confirmed in Hong Kong[2]. It has raised concerns that, based on the large number of mutations in the spike protein and elsewhere on the virus (https://covdb.stanford.edu/page/mutation-viewer/#omicron), this variant will have considerable escape from vaccine elicited immunity[3,4]. Furthermore, several mutations in the receptor binding domain and S2 are predicted to increase transmission[4].

We previously engineered a human lung cell line (H1299-ACE2, Extended Data Fig. 1) to over-express the human ACE2 (hACE2) receptor[5]. We used it here to both isolate Omicron and test neutralization (Materials and methods). Isolation of the Omicron virus was done using two passages in H1299-ACE2, with the second passage a coculture of infected H1299-ACE2 with the Vero E6 African green monkey kidney cell line. Sequencing of the isolated virus confirmed it was the Omicron variant bearing the R346K mutation. We observed no mutations introduced *in vitro* as majority or minority variants (Extended Data Table 1). H1299-ACE2 cells were similar to Vero E6 in the formation of infection foci in a live virus infection with ancestral D614G and Beta variant viruses but were more sensitive than unmodified Vero E6 (Extended Data Fig. 2A-B). Infection by cell-free Omicron of unmodified Vero E6 cells was inefficient (Extended Data Fig. 2C) and we could not use cell-free Omicron infection in Vero E6 cells to generate a useable virus stock of this isolate (Extended Data Fig. 2D).

We observed that Omicron infected the H1299 hACE2-expressing cells in a concentration dependent manner but did not infect the parental H1299, indicating that hACE2 is required for Omicron entry (Fig. 1A-B). We then tested the ability of plasma from BNT162b2 vaccinated study participants to neutralize Omicron versus ancestral D614G virus in a live virus neutralization assay. We tested plasma samples after 2 doses of vaccine from 19 participants (Extended Data Tables 2 and 3), with 6 having no previous record of SARS-CoV-2 infection nor detectable SARS-CoV-2 nucleocapsid antibodies indicative of previous infection (Materials and methods). Samples from a later timepoint were available for two of the vaccinated only participants (Extended Data Table 3) and these were also tested. The previously infected and vaccinated participants were infected with either ancestral SARS-CoV-2 strains or the Delta variant (Extended Data Table 3). To quantify neutralization in the live virus neutralization assay, we calculated the focus reduction neutralization test ($FRNT_{50}$) value, which is the inverse of the plasma dilution required for 50% reduction in infection focus number.

Consistent with previous studies[6-8], we observed that previously infected and vaccinated individuals had higher neutralization capacity of ancestral virus relative to those vaccinated only (Fig. 1C). For all

participants, the ability to neutralize Omicron was lower than ancestral virus (Fig. 1C). Geometric mean titer (GMT) $FRNT_{50}$ for all participants declined from 1963 to 89, a 22-fold drop (Fig. 1D, 95% CI 16-30). The fold drop was 22-fold both in individuals who were previously infected and vaccinated (95% CI 16-34) and vaccinated only (95% CI 15-32, Fig. 1D). Six of the samples showed fitted values for 50% Omicron neutralization which corresponded to a plasma concentration which was higher than the most concentrated plasma tested (a 1:25 dilution). This included the two samples collected at a later timepoint post-vaccination, one of which showed a complete knockout of neutralization activity with Omicron (Extended Data Table 3, Fig. 1C). Excluding these 6 values from the analysis changed the Omicron effect to a 19-fold drop (95% CI 14-25) well within the 95% confidence intervals of the fold-drops for the raw values (Fig. 1D). Interestingly, Omicron virus neutralization by samples from previously infected and vaccinated participants was similar to ancestral virus neutralization by samples from participants vaccinated with 2 doses of BNT162b2 but not previously infected (Fig. 1C). GMT $FRNT_{50}$ for Omicron in the previously infected and vaccinated group was 305 (95% CI 134-695) while GMT $FRNT_{50}$ for ancestral virus in the vaccinated only group was 263 (95% CI 147-472).

We compared these results with neutralization of the Beta variant[5,9-15] using Beta and ancestral virus infection of H1299-ACE2 (Extended Data Fig. 3A) and Vero E6 (Extended Data Fig. 3B) cells. Fold-drop relative to the ancestral D614G virus was 4.3 for H1299-ACE2 and 5.0 for Vero E6. These two cell lines therefore gave similar results and showed that Omicron exhibited approximately 4-fold greater escape relative to Beta in our assays.

Our study was not designed to reliably evaluate vaccine efficacy or protection from severe disease. However, a prediction of vaccine efficacy after a 22-fold drop in neutralization can be made in BNT162b2 vaccinated and vaccinated boosted participants based on data from randomized control trials using a model which relates neutralization level to vaccine efficacy[16,17]. Using this model and the fold-drop observed here on previous datasets (Materials and methods), we predict a vaccine efficacy for preventing Omicron symptomatic infection of 73% (95% CI 58-83%) in vaccinated and boosted individuals and 35% (95% CI 20-50%) for vaccinated only individuals, essentially compromising the ability of the vaccine to protect against infection in the latter but not the former group (Fig. 1E). We note that the predictions are similar to actual vaccine efficacy estimates recently reported in the UK[18].

Shortly after we released results, several other groups reported results[2,19-22] including Pfizer- BioNTech (https://www.businesswire.com/news/home/20211208005542/en/). These results mirror ours, with large fold-drops in neutralization of Omicron by vaccine elicited immunity, neutralizing monoclonal antibodies, and plasma from convalescent individuals infected by other variants. Interestingly, the Pfizer-BioNTech study reports that boosting seems to increase neutralization breath which reduces the fold-drop of Omicron mediated escape, and this has been independently confirmed[20]. We do not see such a qualitative effect in the vaccinated previously infected participants in this study, where we observe similar fold-drops to vaccinated only.

Limitations of this study include the presence of an R346K substitution in our virus stock. This putative escape mutation[23] which may confer moderate antibody resistance (https://jbloomlab.github.io/SARS2_RBD_Ab_escape_maps/escape-calc/), is not found in the majority of Omicron genomes. Also, the timing of sample collection soon after vaccination (Table S2, S3) does not account for the waning of neutralization capacity[24,25].

Thus far, a milder course of Omicron infection was observed in South Africa relative to previous infection waves in terms of reported numbers of ICU and ventilated patients (e.g., https://covid-19dashboard.news24.com/ collated from the National Institute for Communicable Diseases DatCov system). While there may be other, yet unproven, contributing factors to lower pathogenicity[26], pre-existing immunity would be higher in the Omicron wave because of vaccination, as well as immunity elicited by previous infection in one of three preceding infection waves in South Africa[26]. Therefore, the incomplete Omicron escape from previous immunity described here may be an important factor

accounting for the milder course of infection. Despite the extensive neutralization escape of Omicron, residual neutralization levels may still be sufficient to protect from severe disease[16,17]. Other facets of the adaptive immune response elicited by vaccination and previous infection may increase protection. Furthermore, our observation that vaccination combined with previous infection neutralizes Omicron to a similar extent as vaccination without previous infection neutralizes ancestral virus, indicates that protection from symptomatic infection may occur when vaccination is combined with previous infection or boosting. This may explain why Pfizer BNT162b2 vaccination has been shown to substantially decrease the risk of hospital admission due to Omicron infection in South Africa (https://www.discovery.co.za/corporate/health-insights-vaccines-real-world-effectiveness) and supports the use of further vaccination and boosting to combat Omicron.

Materials and methods

Informed consent and ethical statement

Blood samples were obtained after written informed consent from hospitalized adults with PCR-confirmed SARS-CoV-2 infection and/or vaccinated individuals who were enrolled in a prospective cohort study approved by the Biomedical Research Ethics Committee at the University of KwaZulu–Natal (reference BREC/00001275/2020). Use of residual swab sample was approved by the University of the Witwatersrand Human Research Ethics Committee (HREC) (ref. M210752).

Data availability statement

Sequence of outgrown virus has been deposited in GISAID with accession EPI_ISL_7358094. Raw images of the data are available upon reasonable request.

Code availability

The sequence analysis and visualization pipeline is available on GitHub (https://github.com/nextstrain/ncov). Image analysis and curve fitting scripts in MATLAB v.2019b are available on GitHub (https://github.com/sigallab/NatureMarch2021).

Competing interest statement

Salim S. Abdool Karim is a member in the COVID advisory panel for Emerging Markets at Pfizer. The authors declare no other competing interests.

Author contributions

AS, PLM, TdO. and RJL conceived the study. AS, SC, K., TMG. and LJ designed the study and experiments. AvG, PLM, and JNB identified and provided the virus sample. SHH, generated and provided plaque purified Beta variant virus. M-YSM, FK, BIG, MB, KK, and YG set up and managed the cohort and cohort data. SC, LJ, KK, TMG, HT, JES, CS, DGA, GL, DA, MS, YG, ZJ, and KR, performed experiments and sequence analysis with input from AS, TdO, RJL, and JMB. DSK, DC and MPD performed predictions of vaccine efficacy based on the data. AS, SC, PLM, TdO, LJ, KK, WH, SSAK, DSK, MPD, JNB, RJL, M-YSM interpreted data. AS, LJ, DSK, SC, GL, PLM, and MPD prepared the manuscript with input from all authors.

Whole-genome sequencing, genome assembly and phylogenetic analysis

cDNA synthesis was performed on the extracted RNA using random primers followed by gene-specific multiplex PCR using the ARTIC V.3 protocol (https://www.protocols.io/view/covid-19-artic-v3-illumina-library-construction-an-bibtkann). In brief, extracted RNA was converted to cDNA using the Superscript IV First Strand synthesis system (Life Technologies) and random hexamer primers. SARS-CoV-2 whole-genome amplification was performed by multiplex PCR using primers designed using

Primal Scheme (http://primal.zibraproject.org/) to generate 400-bp amplicons with an overlap of 70 bp that covers the 30 kb SARS-CoV-2 genome. PCR products were cleaned up using AmpureXP purification beads (Beckman Coulter) and quantified using the Qubit dsDNA High Sensitivity assay on the Qubit 4.0 instrument (Life Technologies). We then used the Illumina Nextera Flex DNA Library Prep kit according to the manufacturer's protocol to prepare indexed paired-end libraries of genomic DNA. Sequencing libraries were normalized to 4 nM, pooled and denatured with 0.2 N sodium acetate. Then, a 12-pM sample library was spiked with 1% PhiX (a PhiX Control v.3 adaptor-ligated library was used as a control). We sequenced libraries on a 500-cycle v.2 MiSeq Reagent Kit on the Illumina MiSeq instrument (Illumina). We assembled paired-end fastq reads using Genome Detective 1.126 (https://www.genomedetective.com) and the Coronavirus Typing Tool. We polished the initial assembly obtained from Genome Detective by aligning mapped reads to the reference sequences and filtering out low-quality mutations using the bcftools 1.7-2 mpileup method. Mutations were confirmed visually with BAM files using Geneious software (Biomatters). P2 stock was sequenced and confirmed Omicron with the following substitutions: E:T9I,M:D3G,M:Q19E,M:A63T,N:P13L,N:R203K,N:G204R,ORF1a:K856R,ORF1a:L2084I,ORF1a:A2710T, ORF1a:T3255I,ORF1a:P3395H,ORF1a:I3758V,ORF1b:P314L,ORF1b:I1566V,ORF9b:P10S,S:A67V,S:T95I ,S:Y145D,S:L212I,S:G339D,S:R346K,S:S371L,S:S373P,S:S375F,S:K417N,S:N440K,S:G446S,S:S477N,S:T4 78K,S:E484A,S:Q493R,S:G496S,S:Q498R,S:N501Y,S:Y505H,S:T547K,S:D614G,S:H655Y,S:N679K,S:P681 H,S:N764K,S:D796Y,S:N856K,S:Q954H,S:N969K,S:L981F. Deletions: N:E31-,N:R32-,N:S33- ,ORF1a:S2083-,ORF1a:L3674-,ORF1a:S3675-,ORF1a:G3676-,ORF9b:E27-,ORF9b:N28-,ORF9b:A29- ,S:H69-,S:V70-,S:G142-,S:V143-,S:Y144-,S:N211-. Sequence was deposited in GISAID, accession: EPI_ISL_7358094.

SARS-CoV-2 nucleocapsid enzyme-linked immunosorbent assay (ELISA)

2 µg/ml nucleocapsid protein (Biotech Africa; Catalogue number: BA25-P) was used to coat 96-well, high-binding plates and incubated overnight at 4°C. The plates were incubated in a blocking buffer consisting of 5% skimmed milk powder, 0.05% Tween 20, 1x PBS. Plasma samples were diluted to a 1:100 dilution in a blocking buffer and added to the plates. Horseradish peroxidase (HRP) conjugated IgG secondary antibody was diluted to 1:3000 in blocking buffer and added to the plates followed by Tetramethylbenzidine (TMB) peroxidase substrate (Thermo Fisher Scientific). Upon stopping the reaction with 1 M H_2SO_4, absorbance was measured at a 450 nm wavelength.

Cells

Vero E6 cells (ATCC CRL-1586, obtained from Cellonex in South Africa) were propagated in complete growth medium consisting of Dulbecco's Modified Eagle Medium (DMEM) with 10% fetal bovine serum (Hyclone) containing 10mM of HEPES, 1mM sodium pyruvate, 2mM L-glutamine and 0.1mM nonessential amino acids (Sigma-Aldrich). Vero E6 cells were passaged every 3–4 days. H1299 cell lines were propagated in growth medium consisting of complete Roswell Park Memorial Institute (RPMI) 1640 medium with 10% fetal bovine serum containing 10mM of HEPES, 1mM sodium pyruvate, 2mM L-glutamine and 0.1mM nonessential amino acids. H1299 cells were passaged every second day. The H1299-E3 (H1299-ACE2, clone E3) cell line was derived from H1299 (CRL-5803) as described in our previous work[5] and Figure S1. Briefly, vesicular stomatitis virus G glycoprotein (VSVG) pseudotyped lentivirus containing hACE2 was used to spinfect H1299 cells. ACE-2 transduced H1299 cells (containing an endogenously yellow fluorescent protein labelled histone H2AZ gene[27]) were then subcloned at the single cell density in 96-well plates (Eppendorf) in conditioned media derived from confluent cells. After 3 weeks, wells were detached using a 0.25% trypsin-EDTA solution (Gibco) and plated in two replicate plates, where the first plate was used to determine infectivity and the second was stock. The first plate was screened for the fraction of mCherry positive cells per cell clone upon infection with a SARS-CoV-2 mCherry expressing spike pseudotyped lentiviral vector. Screening was performed using a Metamorph-controlled (Molecular Devices, Sunnyvale, CA) Nikon TiE motorized microscope (Nikon Corporation, Tokyo, Japan) with a 20x, 0.75 NA phase objective, 561 nm laser line,

and 607 nm emission filter (Semrock, Rochester, NY). Images were captured using an 888 EMCCD camera (Andor). The clone with the highest fraction of mCherry expression was expanded from the stock plate and denoted H1299-E3. Infectivity was confirmed with mCherry expressing lentivirus by flow cytometry using a BD Fortessa instrument and analyzed using BD FACSDiva Software (BD Biosciences). This clone was used in the outgrowth and focus forming assay. Cell lines have not been authenticated. The cell lines have been tested for mycoplasma contamination and are mycoplasma negative.

Virus expansion

All work with live virus was performed in Biosafety Level 3 containment using protocols for SARS-CoV-2 approved by the Africa Health Research Institute Biosafety Committee. ACE2-expressing H1299-E3 cells were seeded at 4.5×10^5 cells in a 6 well plate well and incubated for 18–20 h. After one DPBS wash, the sub-confluent cell monolayer was inoculated with 500 µL universal transport medium diluted 1:1 with growth medium filtered through a 0.45-µm filter. Cells were incubated for 1 h. Wells were then filled with 3 mL complete growth medium. After 4 days of infection (completion of passage 1 (P1)), cells were trypsinized, centrifuged at 300 rcf for 3 min and resuspended in 4 mL growth medium. Then 2 mL was added to Vero E6 cells that had been seeded at 2×10^5 cells per mL, 5mL total, 18–20 h earlier in a T25 flask (approximately 1:8 donor-to-target cell dilution ratio) for cell-to-cell infection. The coculture of ACE2-expressing H1299-E3 and Vero E6 cells was incubated for 1 h and the flask was then filled with 7 mL of complete growth medium and incubated for 4 days. The viral supernatant (passage 2 (P2) stock) was used for experiments. Further optimization of the viral outgrowth protocol used for subsequent omicron isolates showed that addition of 4 mL instead of 2 mL of infected H1299-E3 cells to Vero E6 cells that had been seeded at 2×10^5 cells per mL, 20 mL total, 18–20 h earlier in a T75 flask gave P2 stocks with substantially higher titers which could detectably infect Vero E6 cells. The Omicron virus isolate is available from the authors contingent on verification that it will be received and used in a Biosafety Level 3 facility.

Live virus neutralization assay

H1299-E3 cells were plated in a 96-well plate (Corning) at 30,000 cells per well 1 day pre-infection. Plasma was separated from EDTA-anticoagulated blood by centrifugation at 500 rcf for 10 min and stored at −80 °C. Aliquots of plasma samples were heat-inactivated at 56 °C for 30 min and clarified by centrifugation at 10,000 rcf for 5 min. Virus stocks were used at approximately 50-100 focus-forming units per microwell and added to diluted plasma. Antibody–virus mixtures were incubated for 1 h at 37 °C, 5% CO2. Cells were infected with 100 µL of the virus–antibody mixtures for 1 h, then 100 µL of a 1X RPMI 1640 (Sigma-Aldrich, R6504), 1.5% carboxymethylcellulose (Sigma-Aldrich, C4888) overlay was added without removing the inoculum. Cells were fixed 18 h post-infection using 4% PFA (Sigma-Aldrich) for 20 min. Foci were stained with a rabbit anti-spike monoclonal antibody (BS-R2B12, GenScript A02058) at 0.5 µg/mL in a permeabilization buffer containing 0.1% saponin (Sigma-Aldrich), 0.1% BSA (Sigma-Aldrich) and 0.05% Tween-20 (Sigma-Aldrich) in PBS. Plates were incubated with primary antibody overnight at 4 °C, then washed with wash buffer containing 0.05% Tween-20 in PBS. Secondary goat anti-rabbit HRP conjugated antibody (Abcam ab205718)was added at 1 µg/mL and incubated for 2 h at room temperature with shaking. TrueBlue peroxidase substrate (SeraCare 5510-0030) was then added at 50 µL per well and incubated for 20 min at room temperature. Plates were imaged in an ImmunoSpot Ultra-V S6-02-6140 Analyzer ELISPOT instrument with BioSpot Professional built-in image analysis (C.T.L).

Statistics and fitting

All statistics and fitting were performed using custom code in MATLAB v.2019b. Neutralization data were fit to:

$Tx=1/1+(D/ID_{50})$.

Here Tx is the number of foci normalized to the number of foci in the absence of plasma on the same plate at dilution D and ID_{50} is the plasma dilution giving 50% neutralization. $FRNT_{50} = 1/ID_{50}$. Values of $FRNT_{50}$ <1 are set to 1 (undiluted), the lowest measurable value. We note that the most concentrated plasma dilution was 1:25 and therefore $FRNT_{50} < 25$ were extrapolated. We have marked these values in Figure 1C and calculate the fold-change $FRNT_{50}$ either for the raw values or for values where $FRNT_{50} > 25$ in Figure 1D.

Estimating vaccine efficacy from neutralization titers

Previously, the fold reduction in neutralization was shown to correlate and predict vaccine efficacy against symptomatic infection with ancestral SARS-CoV-2[17], and more recently with variants of concern[16] in data from RCTs. The model was used here to estimate the vaccine efficacy against Omicron based on the fold-drop observed in this study applied to the RCT data. Briefly, vaccine efficacy (VE) was estimated based on the ($\log_{10}$) fold-drop in neutralization titer to Omicron (f), and the ($\log_{10}$) mean neutralization titer as a fold of the mean convalescent titer reported for BNT162b2 in phase 1/2 trials (μ) using the equation:

$$VE(\mu, f) = \int_{-\infty}^{\infty} N(x, \mu - f, \sigma) \frac{1}{1 + e^{-k(x - x_{50})}}\, dx.$$

Here, N is the probability density function of a normal distribution with mean $\mu - f$ and standard deviation σ, and k and x_{50} are the parameters of the logistic function relating neutralization to protection for the Pfizer-BNT162b2 vaccine which were fitted from RCT data: $\sigma = 0.46$, $k = 3$ and $x_{50} = \log_{10} 0.2$ for symptomatic infection[17]. Importantly, $\mu = \log_{10} 2.4$ for trial participants vaccinated with two doses of BNT162b2, and $\mu = \log_{10} 12$ for vaccinated and boosted trial participants[16,17].

Acknowledgements

This study was supported by the Bill and Melinda Gates award INV-018944 (AS), National Institutes of Health award R01 AI138546 (AS), and South African Medical Research Council awards (AS, TdO, PLM) and the UK Foreign, Commonwealth and Development Office and Wellcome Trust (Grant no 221003/Z/20/Z, PLM). PLM is also supported by the South African Research Chairs Initiative of the Department of Science and Innovation and the NRF (Grant No 98341). DSK, DC, and MPD are supported by NHMRC (Australia) Fellowship / Investigator grants. DA was supported by the European and Developing Countries Clinical Trials Partnership (EDCTP) Senior Fellowship (Grant No TMA2017SF-1960). The funders had no role in study design, data collection and analysis, decision to publish, or preparation of the manuscript.

References

1 Pulliam, J. R. C. *et al.* Increased risk of SARS-CoV-2 reinfection associated with emergence of the Omicron variant in South Africa. *medRxiv*, 2021.2011.2011.21266068, doi:10.1101/2021.11.11.21266068 (2021).

2 Lu, L. *et al.* Neutralization of SARS-CoV-2 Omicron variant by sera from BNT162b2 or Coronavac vaccine recipients. *medRxiv*, 2021.2012.2013.21267668, doi:10.1101/2021.12.13.21267668 (2021).

3 Harvey, W. T. *et al.* SARS-CoV-2 variants, spike mutations and immune escape. *Nature Reviews Microbiology* **19**, 409-424, doi:10.1038/s41579-021-00573-0 (2021).

4 Tao, K. *et al.* The biological and clinical significance of emerging SARS-CoV-2 variants. *Nature Reviews Genetics* **22**, 757-773, doi:10.1038/s41576-021-00408-x (2021).

5 Cele, S. *et al.* Escape of SARS-CoV-2 501Y.V2 from neutralization by convalescent plasma. *Nature* **593**, 142-146, doi:10.1038/s41586-021-03471-w (2021).

6 Keeton, R. *et al.* Prior infection with SARS-CoV-2 boosts and broadens Ad26.COV2.S immunogenicity in a variant-dependent manner. *Cell Host Microbe* **29**, 1611-1619 e1615, doi:10.1016/j.chom.2021.10.003 (2021).

7 Stamatatos, L. *et al.* (American Association for the Advancement of Science, 2021).

8 Ebinger, J. E. *et al.* Antibody responses to the BNT162b2 mRNA vaccine in individuals previously infected with SARS-CoV-2. *Nature Medicine* **27**, 981-984, doi:10.1038/s41591-021-01325-6 (2021).

9 Tegally, H. *et al.* Detection of a SARS-CoV-2 variant of concern in South Africa. *Nature* **592**, 438-443, doi:10.1038/s41586-021-03402-9 (2021).

10 Garcia-Beltran, W. F. *et al.* Multiple SARS-CoV-2 variants escape neutralization by vaccine-induced humoral immunity. *Cell* **184**, 2372-2383. e2379 (2021).

11 Wibmer, C. K. *et al.* SARS-CoV-2 501Y.V2 escapes neutralization by South African COVID-19 donor plasma. *Nat Med* **27**, 622-625, doi:10.1038/s41591-021-01285-x (2021).

12 Zhou, D. *et al.* Evidence of escape of SARS-CoV-2 variant B.1.351 from natural and vaccine-induced sera. *Cell* **184**, 2348-2361 e2346, doi:10.1016/j.cell.2021.02.037 (2021).

13 Planas, D. *et al.* Sensitivity of infectious SARS-CoV-2 B.1.1.7 and B.1.351 variants to neutralizing antibodies. *Nat Med* **27**, 917-924, doi:10.1038/s41591-021-01318-5 (2021).

14 Wang, P. *et al.* Antibody resistance of SARS-CoV-2 variants B.1.351 and B.1.1.7. *Nature* **593**, 130-135, doi:10.1038/s41586-021-03398-2 (2021).

15 Wang, Z. *et al.* mRNA vaccine-elicited antibodies to SARS-CoV-2 and circulating variants. *Nature* **592**, 616-622, doi:10.1038/s41586-021-03324-6 (2021).

16 Cromer, D. *et al.* Neutralising antibody titres as predictors of protection against SARS-CoV-2 variants and the impact of boosting: a meta-analysis. *The Lancet Microbe* (2021).

17 Khoury, D. S. *et al.* Neutralizing antibody levels are highly predictive of immune protection from symptomatic SARS-CoV-2 infection. *Nature medicine*, 1-7 (2021).

18 Andrews, N. *et al.* Effectiveness of COVID-19 vaccines against the Omicron (B.1.1.529) variant of concern. *medRxiv*, 2021.2012.2014.21267615, doi:10.1101/2021.12.14.21267615 (2021).

19 Wilhelm, A. *et al.* Reduced Neutralization of SARS-CoV-2 Omicron Variant by Vaccine Sera and monoclonal antibodies. *medRxiv*, 2021.2012.2007.21267432, doi:10.1101/2021.12.07.21267432 (2021).

20 Garcia-Beltran, W. F. *et al.* mRNA-based COVID-19 vaccine boosters induce neutralizing immunity against SARS-CoV-2 Omicron variant. *medRxiv*, 2021.2012.2014.21267755, doi:10.1101/2021.12.14.21267755 (2021).

21 Rössler, A., Riepler, L., Bante, D., Laer, D. v. & Kimpel, J. SARS-CoV-2 B.1.1.529 variant (Omicron) evades neutralization by sera from vaccinated and convalescent individuals. *medRxiv*, 2021.2012.2008.21267491, doi:10.1101/2021.12.08.21267491 (2021).

22 Cao, Y. *et al.* B.1.1.529 escapes the majority of SARS-CoV-2 neutralizing antibodies of diverse epitopes. *bioRxiv*, 2021.2012.2007.470392, doi:10.1101/2021.12.07.470392 (2021).
23 Weisblum, Y. *et al.* Escape from neutralizing antibodies by SARS-CoV-2 spike protein variants. *Elife* **9**, e61312 (2020).
24 Goldberg, Y. *et al.* Waning immunity of the BNT162b2 vaccine: A nationwide study from Israel. *medRxiv*, 2021.2008.2024.21262423, doi:10.1101/2021.08.24.21262423 (2021).
25 Chemaitelly, H. *et al.* Waning of BNT162b2 vaccine protection against SARS-CoV-2 infection in Qatar. *New England Journal of Medicine* (2021).
26 Cele, S. *et al.* SARS-CoV-2 evolved during advanced HIV disease immunosuppression has Beta-like escape of vaccine and Delta infection elicited immunity. *medRxiv*, 2021.2009.2014.21263564, doi:10.1101/2021.09.14.21263564 (2021).
27 Sigal, A. *et al.* Variability and memory of protein levels in human cells. *Nature* **444**, 643-646, doi:10.1038/nature05316 (2006).

Fig. 1

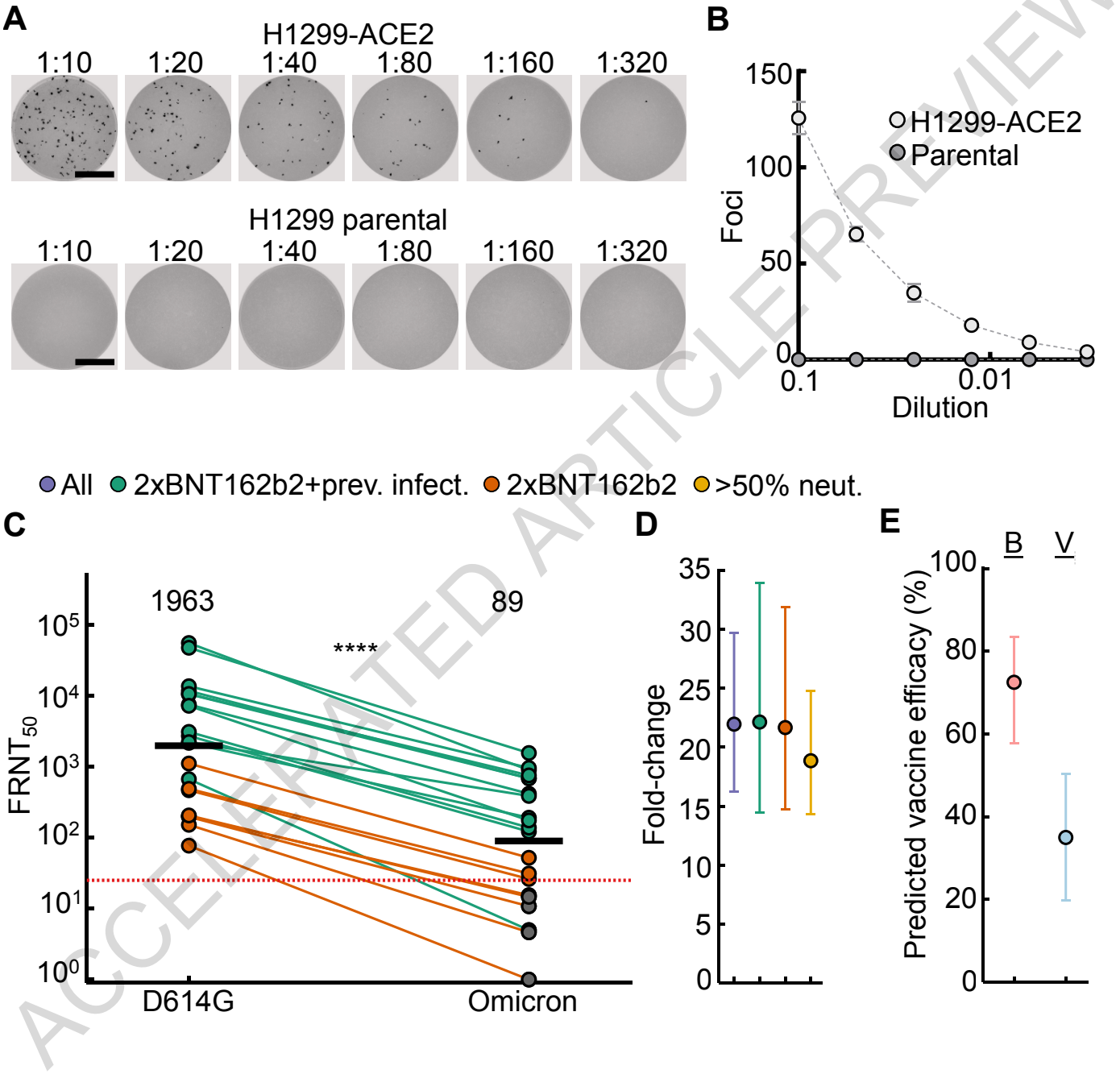

Figure legend

Figure 1: ACE2 dependence and neutralization of the Omicron variant by Pfizer BNT162b2 elicited immunity. (A) Representative images of infection foci in wells of a multi-well plate in a titration of live SARS-CoV-2 Omicron virus on H1299-ACE2 and H1299 parental cells. Numbers above well images denote viral stock dilution. Scale bar is 2mm. (B) Quantified number of foci as a function of Omicron virus stock dilution. Mean and standard deviation of 6 replicates from 2 independent experiments. (C) Neutralization of Omicron virus compared to D614G ancestral virus by plasma from participants vaccinated with two doses of BNT162b2 and previously SARS-CoV-2 infected (green) or uninfected (orange). Numbers in black above each virus strain are geometric mean titers (GMT) of the reciprocal plasma dilution ($FRNT_{50}$) resulting in 50% reduction in infection foci. Red horizontal line denotes most concentrated plasma used. 21 samples were tested from n=19 participants in 2 independent experiments (n=13 vaccinated and previously infected and n=6 vaccinated only). Grey points denote measurements where 50% neutralization was not achieved with the most concentrated plasma used. $p=4.8 \times 10^{5}$ as determined by the Wilcoxon rank sum test. (D) Geometric means and 95% confidence intervals of fold-changes between ancestral D614G and Omicron neutralization. Purple denotes all participants, green denotes vaccinated previously infected, orange denotes vaccinated only, and yellow denotes all participants excluding those where 50% neutralization was not achieved. (E) Predicted vaccine efficacy and 95% confidence intervals against symptomatic infection using previous data from RCTs and the 22-fold drop observed in this study. Predictions are for boosted (B, red) or vaccinated only (V, blue).

Extended Data Fig. 1

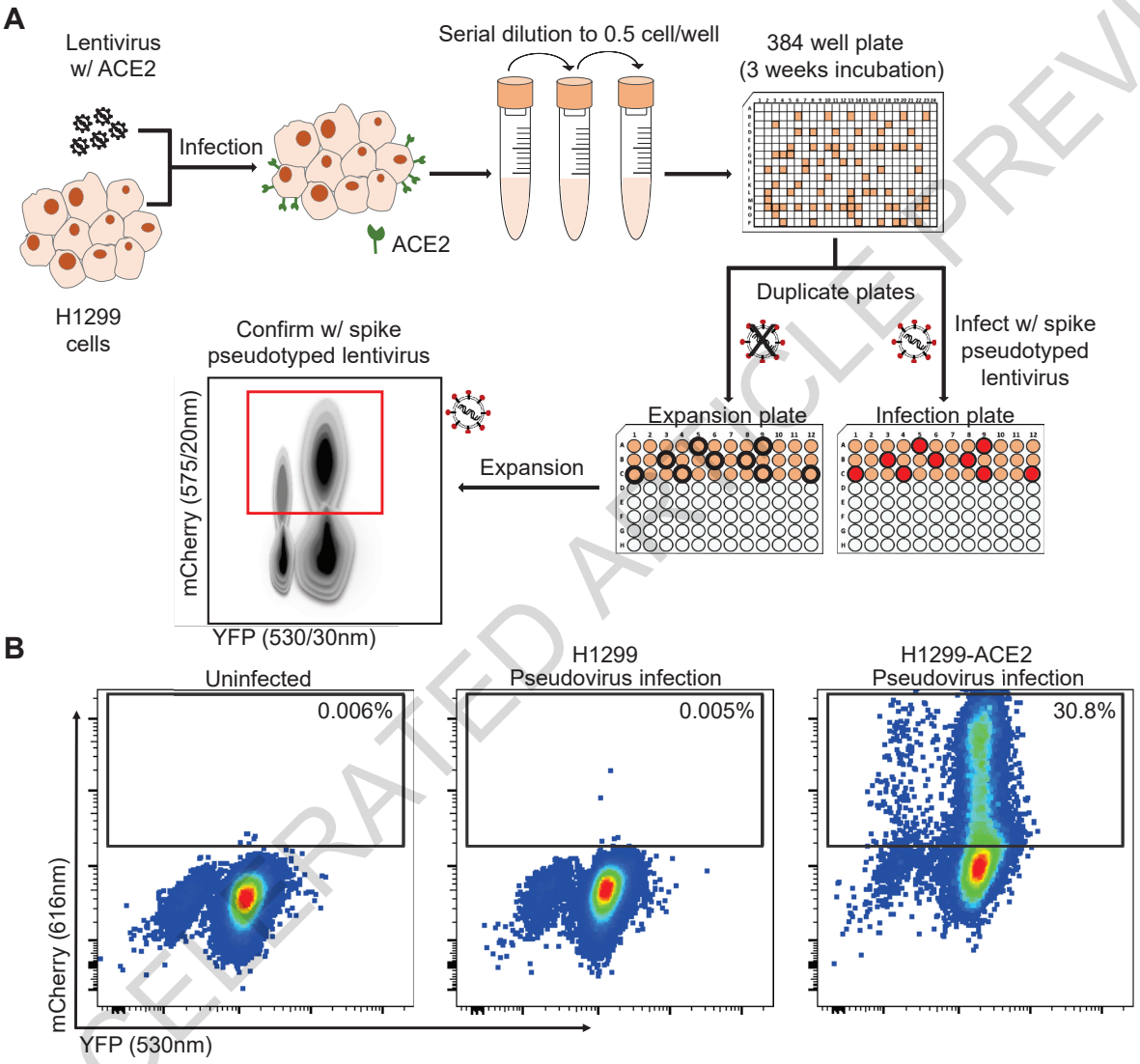

Supplementary Figure legends

Extended Data Figure 1: Generation of H1299-ACE2 clonal cell line. (A) The H1299 human non-small cell lung carcinoma cell line with YFP labelled histone H2AZ was spinfected with the pHAGE2-EF1a-Int-ACE2 lentivector. Cells were single cell cloned by limiting dilution in a 384-well plate. Clones were expanded into duplicate 96-well plates, where one plate was used to select infectable clones based on mCherry signal from infection with SARS-CoV-2 mCherry expressing spike pseudotyped lentivirus. Clones were chosen based on infectability and expanded from the non-infected replicate 96-well plate. (B) Flow cytometry of SARS-CoV-2 mCherry expressing spike pseudotyped lentivirus infection in H1299-ACE2 cells versus H1299 parental cells.

Extended Data Fig. 2

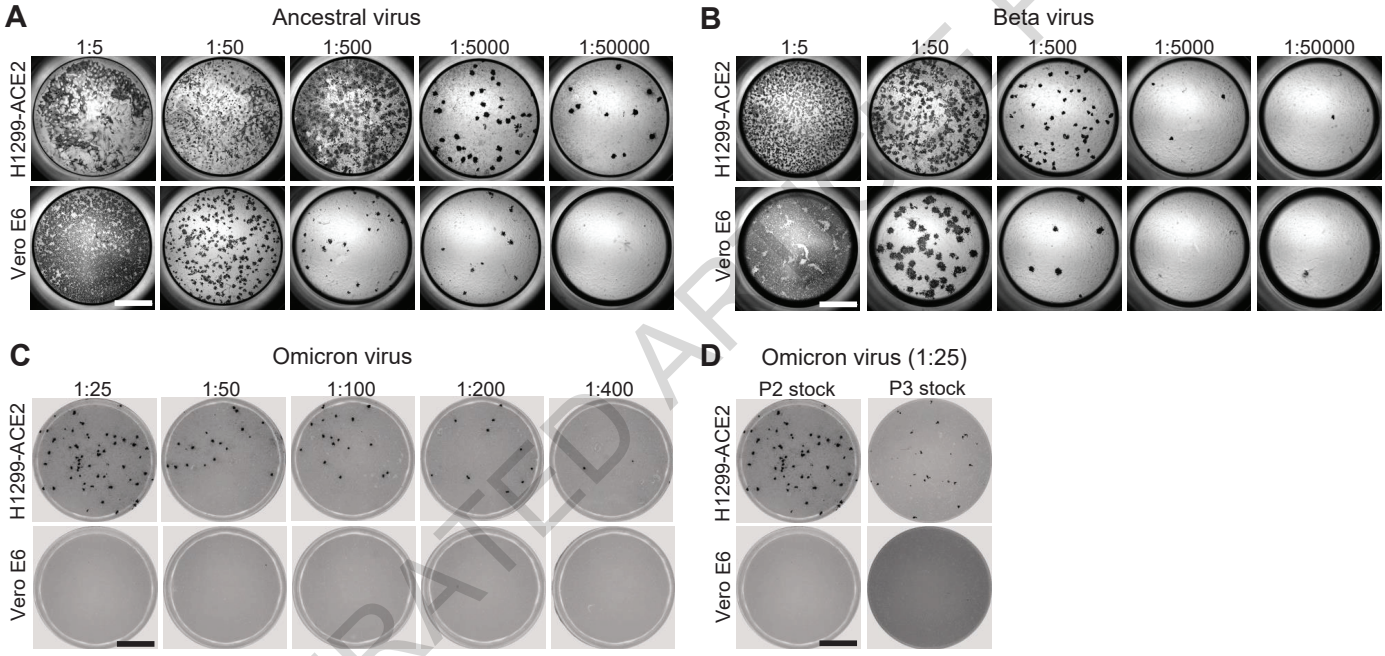

Extended Data Figure 2: Comparison of SARS-CoV-2 infection in H1299-ACE2 and Vero E6 cells. Both H1299-ACE2 and Vero E6 cells were infected with the same viral stock in the same experiment with D614G virus (A) or Beta virus (B) and a focus forming assay was performed. (C) Focus forming assay with stock of Omicron virus isolate on H1299-ACE2 and Vero E6 cells. (D) Comparison of passage 2 (P2) and passage 3 (P3) stock, where P3 stock was generated by infection of 1 mL of cell-free P2 stock in 20 mL of Vero E6 cells seeded at $2x10^5$ cells per mL and incubated over 4 days. Numbers above well images denote viral stock dilution. Scale bar is 2mm.

Extended Data Fig. 3

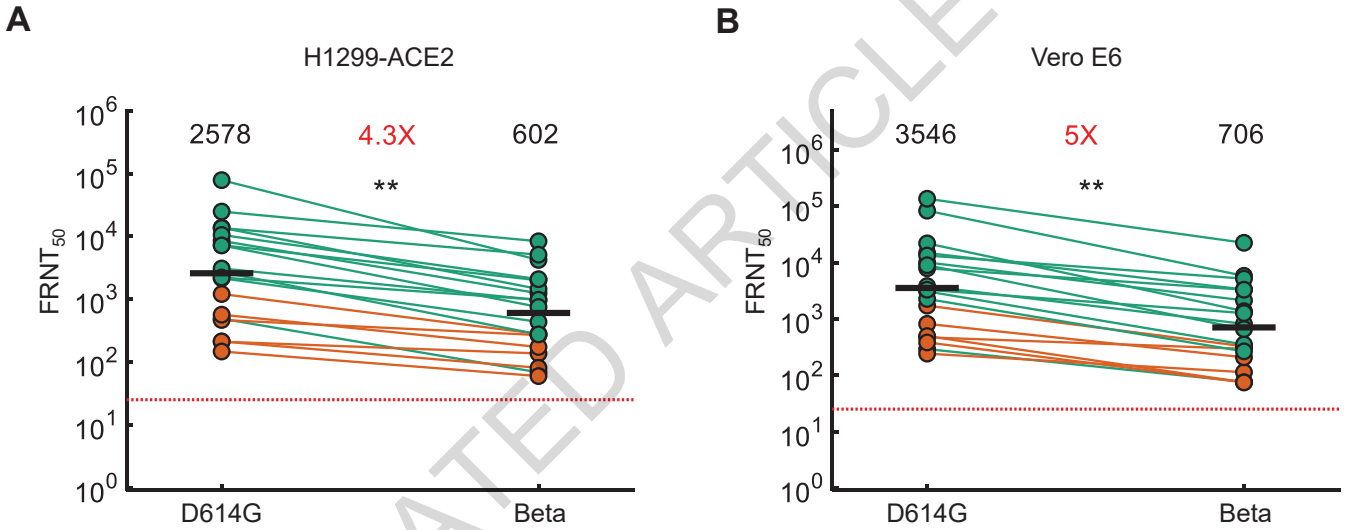

Extended Data Figure S3: Neutralization of the Beta variant by Pfizer BNT162b2 elicited immunity. Neutralization of the Beta variant virus compared to D614G ancestral virus in H1299-ACE2 (A) or Vero E6 cells (B) in participants vaccinated with BNT162b2 and infected by SARS-CoV-2 (green) or vaccinated only (orange). Numbers in black above each virus strain are geometric mean titers (GMT) of the reciprocal plasma dilution (FRNT50) resulting in 50% reduction in the number of infection foci. Numbers in red denote fold-change in GMT between virus strain on the left and the virus strain on the right of each panel. Red horizontal line denotes most concentrated plasma used. Samples were tested from the n=19 participants described in Table S2 and S3, where n=6 were vaccinated only and n=13 were vaccinated and previously infected. p=0.006 for both (A) and (B) as determined by the Wilcoxon rank sum test.

Extended Data Table 1

Amino Acid Change	Nucleotide Change	Codon(s) Change	K032623_N67
A67V	21762C>T	21761 GCT>GTT	GCT - 0 GTT - 133
***H69_V70del**	21766_21771delACATGT	21766_21771ACATGT >del	ACATGT - 0 del - 123
T95I	21846C>T	21845 ACT>ATT	ACT - 0 ATT - 164
***G142D**	21987_21989delGTG	21987_21989GTG >del	GTG - 0 del - 432
***V143_Y145del**	21990_21995delTTTATT	21990_21995TTTATT >del	TTTATT - 0 del - 432
***L212I**	22194_22196delATT	22194_22196ATT >del	ATT - 0 del - 146
***R214_D215**	22204_22205insGAGCCAGAA	22204_22205GAGCCAGAA >ins	WT - 37 insGAGCCAGAA - 74
G339D	22578G>A	22577 GGT>GAT	GGT - 0 GAT - 255
R346K	22599G>A	22598 AGA>AAA	AGA - 1 AAA - 250
S371L	22674C>T	22674 TCC>CTC	TCC - 0 CTC - 152
S373P	22679T>C	22679 TCA>CCA	TCA - 3 CCA - 166
S375F	22686C>T	22685 TCC>TTC	TCC - 0 TTC - 160
K417T	22813G>T	22811 AAG>AAT	AAG – 3 AAT – 934
N440K	22882T>G	22880 AAT>AAG	AAT – 3 AAG – 791
G446S	22898G>A	22898 GGT>AGT	GGT – 30 AGT – 870
T478K	22995C>A	22994 ACA>AAA	ACA - 0 AAA - 59
E484A	23013A>C	23012 GAA>GCA	GAA - 0 GCA - 110
Q493R	23040A>G	23039 CAA>CGA	CAA - 0 CGA - 128

Extended Data Table 1 (cont'd)

Amino Acid Change	Nucleotide Change	Codon(s) Change	K032623_N67
G496S	23048G>A	23048 GGT>AGT	GGT - 0 AGT - 150
Q498R	23055A>G	23054 CAA>CGA	CAA - 1 CGA - 144
N501Y	23063A>T	23063 AAT>TAT	AAT - 0 TAT - 209
Y505H	23075T>C	23075 TAC>CAC	TAC - 1 CAC - 261
T547K	23202C>A	23201 ACA>AAA	ACA - 0 AAA - 777
D614G	23403A>G	23402 GAT>GGT	GAT - 1 GGT - 1803
H655Y	23525C>T	23525 CAT>TAT	CAT - 3 TAT - 1639
N679K	23599T>G	23597 AAT>AAG	AAT - 1 AAG - 682
P681H	23604C>A	23603 CCT>CAT	CCT - 0 CAT - 535
Q954H	24424A>T	24422 CAA>CAT	CAA - 1 CAT - 753
N969K	24469T>A	24467 AAT>AAA	AAT - 0 AAA - 1692
L981F	24503C>T	24503 CTT>TTT	CTT - 0 TTT - 1797

Extended Data Table 1: Codon frequency table

This table shows the amino acid change, the nucleotide position of the genome, codon change and the frequency of the codon on the assembled genome.

*Only deletions or insertion where the adjacent codon was preserved were counted; WT - Wild Type, i.e reads without the insertion.

Extended Data Table 2

	All	Vaccinated only	Infected and vaccinated
Number of Participants	19	6	13
Age (years)	52 (39-67)	54 (36-71)	51 (45-63)
Days post-vaccination	26 (14-33)	14.5 (8.5-37.5)	28 (18-32)
Days post-infection			379 (127-468)
Days post-infection to vaccination			353 (114-444)
Date range of symptom onset			Jun 2020 – Jul 2021
Male sex	7	2	5

Extended Data Table 2: Summary table of participants

All values are median (IQR) and inclusive of all samples used (early and late timepoints for 2 participants).

Extended Data Table 3

Sample	Participant	Age	Sex	Days post 2nd vaccination dose	Days diagnostic swab to sample	Date symptom onset or diagnostic test	Infecting virus*	$FRNT_{50}$ D614G	$FRNT_{50}$ Omicron
1	1	60-69	F	10	-	-	-	196	10.8
2	2	70-79	M	10	-	-	-	463	26.1
3	2	70-79	M	45	-	-	-	205	14.6
4	3	30-39	M	14	-	-	-	485	31.1
5	4	70-79	F	10	-	-	-	199	15.4
6	4	70-79	F	48	-	-	-	76.8	1.0
7	5	30-39	F	10	-	-	-	1102	51.9
8	6	30-39	F	33	-	-	-	151	4.6
9	7	40-49	F	14	458	Jul-2020	Ancestral	10447	681
10	8	60-69	F	63	468	Jul-2020	Ancestral	7468	414
11	9	20-29	F	31	487	Aug-2020	Ancestral	2153	190
12	10	20-29	M	37	493	Jul-2020	Ancestral	2697	121
13	11	60-69	F	28	378	Jul-2020	Ancestral	54823	892
14	12	60-69	M	26	379	Jul-2020	Ancestral	47023	1550
15	13	40-49	F	32	479	Aug-2020	Ancestral	13517	955
16	14	50-59	M	30	370	Sep-2020	Ancestral	11590	681
17	15	40-49	F	22	456**	Jun-2020**	Ancestral/Delta	664	5.0
18	16	40-49	M	18	83	Jul-2021***	Delta	10511	749
19	17	70-79	M	37	8	Jul-2021	Delta	3074	138
20	18	50-59	F	13	127	Jul-2021***	Delta	2205	385
21	19	60-69	F	14	103	Jul-2021	Delta	7160	174

Extended Data Table 3: Participant information per sample

*Determined by infection wave in South Africa. First infection wave (April-October 2020) consisted of ancestral strains with the D614G mutation. Third infection wave (April-October 2021) was dominated by the Delta variant. **Participant reinfected during Delta infection wave, sample is taken 3 months post-recovery of Delta infection. Asymptomatic during reinfection.
***Asymptomatic.

Consortia

Network for Genomic Surveillance in South Africa (NGS-SA)

Mary-Ann Davies[17], Marvin Hsiao[18], Darren Martin[12,19], Koleka Mlisana[20,21], Constantinos Kurt Wibmer[4], Carolyn Williamson[4,12,22] & Denis York[23].

[17]Center for Infectious Disease Epidemiology and Research, School of Public Health and Family Medicine, University of Cape Town, Cape Town, South Africa. [18]University of Cape Town/Groote Schuur Complex of the National Health Laboratory Service (NHLS), University of Cape Town, Cape Town, South Africa. [19]Division of Computational Biology, Department of Integrative Biomedical Sciences, University of Cape Town, Cape Town, South Africa. [20]Medical Microbiology Department, University of KwaZulu-Natal, Durban, South Africa. [21]National Health Laboratory Services (NHLS), Durban, South Africa. [22]Wellcome Centre for Infectious Diseases Research in Africa, University of Cape Town, Cape Town, South Africa. [23]Molecular Diagnostics Services, Durban, South Africa.

COMMIT-KZN Team

Rohen Harrichandparsad[24], Kobus Herbst[1,25], Prakash Jeena[26], Thandeka Khoza[1], Henrik Kløverpris[1,27], Alasdair Leslie[1,11], Rajhmun Madansein[28], Nombulelo Magula[29], Nithendra Manickchund[13], Mohlopheni Marakalala[1,11], Matilda Mazibuko[1], Mosa Moshabela[30], Ntombifuthi Mthabela[1], Kogie Naidoo[8], Zaza Ndhlovu[1, 31], Thumbi Ndung'u[1,16,31,32], Nokuthula Ngcobo[1], Kennedy Nyamande[33], Vinod Patel[34], Theresa Smit[1], Adrie Steyn[1,35] & Emily Wong[1,35].

[24]Department of Neurosurgery, University of KwaZulu-Natal, Durban, South Africa. [25]South African Population Research Infrastructure Network, Durban, South Africa. [26]Department of Paediatrics and Child Health, University of KwaZulu-Natal, Durban, South Africa. [27]Department of Immunology and Microbiology, University of Copenhagen, Copenhagen, Denmark. [28]Department of Cardiothoracic Surgery, University of KwaZulu-Natal, Durban, South Africa. [29]Department of Medicine, King Edward VIII Hospital and University of KwaZulu Natal, Durban, South Africa.[30]College of Health Sciences, University of KwaZulu-Natal, Durban, South Africa. [31]Ragon Institute of MGH, MIT and Harvard, Boston, USA. [32]HIV Pathogenesis Programme, The Doris Duke Medical Research Institute, University of KwaZulu-Natal, Durban, South Africa. [33]Department of Pulmonology and Critical Care, University of KwaZulu-Natal, Durban, South Africa. [34]Department of Neurology, University of KwaZulu-Natal, Durban, South Africa.[35]Division of Infectious Diseases, University of Alabama at Birmingham, USA.

nature portfolio

Corresponding author(s): Alex Sigal

Last updated by author(s): Dec 17, 2021

Reporting Summary

Nature Portfolio wishes to improve the reproducibility of the work that we publish. This form provides structure for consistency and transparency in reporting. For further information on Nature Portfolio policies, see our Editorial Policies and the Editorial Policy Checklist.

Statistics

For all statistical analyses, confirm that the following items are present in the figure legend, table legend, main text, or Methods section.

n/a	Confirmed
☐	☒ The exact sample size (*n*) for each experimental group/condition, given as a discrete number and unit of measurement
☐	☒ A statement on whether measurements were taken from distinct samples or whether the same sample was measured repeatedly
☐	☒ The statistical test(s) used AND whether they are one- or two-sided *Only common tests should be described solely by name; describe more complex techniques in the Methods section.*
☒	☐ A description of all covariates tested
☒	☐ A description of any assumptions or corrections, such as tests of normality and adjustment for multiple comparisons
☐	☒ A full description of the statistical parameters including central tendency (e.g. means) or other basic estimates (e.g. regression coefficient) AND variation (e.g. standard deviation) or associated estimates of uncertainty (e.g. confidence intervals)
☐	☒ For null hypothesis testing, the test statistic (e.g. *F*, *t*, *r*) with confidence intervals, effect sizes, degrees of freedom and *P* value noted *Give P values as exact values whenever suitable.*
☒	☐ For Bayesian analysis, information on the choice of priors and Markov chain Monte Carlo settings
☒	☐ For hierarchical and complex designs, identification of the appropriate level for tests and full reporting of outcomes
☒	☐ Estimates of effect sizes (e.g. Cohen's *d*, Pearson's *r*), indicating how they were calculated

Our web collection on statistics for biologists contains articles on many of the points above.

Software and code

Policy information about availability of computer code

Data collection	No code used
Data analysis	All statistics and fitting were performed using MATLAB v.2019b.

For manuscripts utilizing custom algorithms or software that are central to the research but not yet described in published literature, software must be made available to editors and reviewers. We strongly encourage code deposition in a community repository (e.g. GitHub). See the Nature Portfolio guidelines for submitting code & software for further information.

Data

Policy information about availability of data

All manuscripts must include a data availability statement. This statement should provide the following information, where applicable:

- Accession codes, unique identifiers, or web links for publicly available datasets
- A description of any restrictions on data availability
- For clinical datasets or third party data, please ensure that the statement adheres to our policy

Sequence was deposited in GISAID, accession: EPI_ISL_7358094. All data are contained in the manuscript.

Field-specific reporting

Please select the one below that is the best fit for your research. If you are not sure, read the appropriate sections before making your selection.

☒ Life sciences ☐ Behavioural & social sciences ☐ Ecological, evolutionary & environmental sciences

For a reference copy of the document with all sections, see nature.com/documents/nr-reporting-summary-flat.pdf

Life sciences study design

All studies must disclose on these points even when the disclosure is negative.

Sample size	Sample size was not pre-determined. We used all the samples we had available which met the inclusion/exclusion criteria.
Data exclusions	We excluded samples from PfizerBNT162b2 vaccinated participants who were previously infected with the Beta variant since we wanted to compare to the Omicron to Beta virus neutralization. We excluded samples positive for SARS-CoV-2 nucleocapsid (ie previously infected) where we could not determine the infecting variant/strain by a time of infection.
Replication	Repeated in an independent experiment on a different day. Geometric mean of replicate samples was used.
Randomization	Groups were determined based on whether
Blinding	No blinding.

Reporting for specific materials, systems and methods

We require information from authors about some types of materials, experimental systems and methods used in many studies. Here, indicate whether each material, system or method listed is relevant to your study. If you are not sure if a list item applies to your research, read the appropriate section before selecting a response.

Materials & experimental systems

n/a	Involved in the study
☐	☒ Antibodies
☐	☒ Eukaryotic cell lines
☒	☐ Palaeontology and archaeology
☒	☐ Animals and other organisms
☐	☒ Human research participants
☒	☐ Clinical data
☒	☐ Dual use research of concern

Methods

n/a	Involved in the study
☒	☐ ChIP-seq
☐	☒ Flow cytometry
☒	☐ MRI-based neuroimaging

Antibodies

Antibodies used	Foci were stained with a rabbit anti-spike monoclonal antibody (BS-R2B12, GenScript A02058) at 0.5 µg/mL. Secondary goat anti-rabbit horseradish peroxidase (Abcam ab205718) antibody was added at 1 µg/mL
Validation	Information sheet for A02058 at https://www.genscript.com/antibody/A02058-MonoRab_SARS_CoV_2_Spike_S1_Antibody_BS_R2B12_mAb_Rabbit.html. Information sheet for ab205718: https://www.abcam.com/goat-rabbit-igg-hl-hrp-ab205718.html

Eukaryotic cell lines

Policy information about cell lines

Cell line source(s)	Vero E6 cells (ATCC CRL-1586) obtained from Cellonex in South Africa. The H1299-E3 cell line was derived from H1299 (CRL-5803) as described in (2) and Figure S1. H1299 cells were a gift from M. Oren, Weizmann Institute of Science.
Authentication	Cell lines have not been authenticated.
Mycoplasma contamination	The cell lines have been tested for mycoplasma contamination and are mycoplasma negative.
Commonly misidentified lines (See ICLAC register)	None.

Human research participants

Policy information about studies involving human research participants

Population characteristics	Participant characteristics are summarized in Table S1 and listed per participant in Table S2.
Recruitment	Blood samples were obtained from hospitalized adults with PCR-confirmed SARS-CoV-2 infection and/or vaccinated individuals who were enrolled in a prospective cohort study approved by the Biomedical Research Ethics Committee at the University of KwaZulu–Natal.
Ethics oversight	Study approved by the Biomedical Research Ethics Committee at the University of KwaZulu–Natal (reference BREC/00001275/2020). Use of residual swab sample was approved by the University of the Witwatersrand Human Research Ethics Committee (HREC) (ref. M210752).

Note that full information on the approval of the study protocol must also be provided in the manuscript.

Flow Cytometry

Plots

Confirm that:

☒ The axis labels state the marker and fluorochrome used (e.g. CD4-FITC).

☒ The axis scales are clearly visible. Include numbers along axes only for bottom left plot of group (a 'group' is an analysis of identical markers).

☒ All plots are contour plots with outliers or pseudocolor plots.

☒ A numerical value for number of cells or percentage (with statistics) is provided.

Methodology

Sample preparation	Plasma was separated from EDTA-anticoagulated blood by centrifugation at 500 rcf for 10 min and stored at −80°C. Aliquots of plasma samples were heat-inactivated at 56°C for 30 min and clarified by centrifugation at 10,000 rcf for 5 min.
Instrument	Plates were imaged in an ImmunoSpot Ultra-V S6-02-6140 Analyzer ELISPOT instrument with BioSpot Professional built-in image analysis (C.T.L).
Software	BioSpot Professional built-in image analysis (C.T.L).
Cell population abundance	H1299-E3 clone was previously generated and described. Abundance of infected cells with lentiviral infection was 30%/
Gating strategy	H1299-E3 clone was previously generated and described. Gating was based on FSC/SSC for live cells, then uninfected cells were used to determine mCherry positive gating.

☒ Tick this box to confirm that a figure exemplifying the gating strategy is provided in the Supplementary Information.